5-2023

Micro-Faraday Cage Design and Analysis for RF Sensitive Components on an LTCC Substrate in HFSS

Roberto Quezada
University of Arkansas, Fayetteville

Micro-Faraday Cage Design and Analysis for RF Sensitive Components on an LTCC Substrate in HFSS

An undergraduate honor thesis submitted in partial fulfillment of the requirements for the Honors Studies in Electrical Engineering

by

Roberto Quezada
Bachelor of Science in Electrical Engineering

University of Arkansas

May 2023

Honeywell Federal Manufacturing & Technologies, LLC operates the Kansas City National Security Campus for the United States Department of Energy / National Nuclear Security Administration under Contract Number DE-NA0002839

Abstract

This thesis focuses on creating and testing two different simulation environments in HFSS and analyzing the effectiveness of a micro-Faraday Cage on the RF Sensitive component by exchanging the SMPS and RF Sensitive component with 25GHz Microstrip Patch Antennas. Modern integrated circuit board systems consist of components that can generate electromagnetic signals and components that may be sensitive to electromagnetic interference. A switched-mode power supply (SMPS) is one component capable of producing electromagnetic interference (EMI) through its fundamental and harmonic switching frequency. By using a Faraday Cage to shield the RF-sensitive element, it is possible to reduce its susceptibility to EMI from other systems and retain the signal's integrity. To develop the micro-Faraday cage, HFSS can be used to create a simulation environment to design a micro-Faraday cage in an LTCC (Low-Temperature Co-Fired Ceramics) substrate as LTCC allows components to be embedded within the substrate. The initial dimensions were 40mm x 40mm x 10mm but then the height was reduced to 0.254 mm (10 mil) to cut down on sim run time. After corrections, The Micro Faraday cage was shown to attenuate the signal in both two and three antenna systems when compared to the antenna that was surrounded only by the core material which only experienced a minor loss. This preliminary data shows promising results for the effectiveness of the MFC however before an affirmative decision can be made on the Micro-Faraday Cage's effectiveness more trials need to be done using different cage configurations and alternate antenna positioning.

Acknowledgments

Principal Investigators: Dr. Samir El-Ghazaly and Dr. Alan Mantooth.

Special thank you to Latarence Butts, and the Electrical Engineering Department at the University of Arkansas for their support.

This work is funded by the Department of Energy's Kansas City National Security Campus, operated by Honeywell Federal Manufacturing & Technologies, LLC, under contract number DE-NA0002839.

Table of Contents:

Honeywell Federal Manufacturing & Technologies, LLC operates the Kansas City National Security Campus for the United States Department of Energy / National Nuclear Security Administration under Contract Number DE-NA0002839

List of Figures:

Introduction:

Modern integrated circuit board systems consist of components that can generate electromagnetic signals and components that may be sensitive to electromagnetic interference. A switched-mode power supply (SMPS) is one such component capable of producing electromagnetic interference (EMI) through its fundamental and harmonic switching frequency. [1] Unlike linear regulators, an SMPS uses switching regulators to efficiently switch between states to convert AC to DC or DC to DC. An IC chip is one type of component that is susceptible to the EMI generated by these noisy components. [1] EMI can disrupt the natural function and can lower signal integrity when the signal in an IC experiences electromagnetic interference or crosstalk. [6] Crosstalk in an IC can cause signal propagation delay or failure. [6] If the susceptible component were to be isolated from EMI, then the power supply and chip would be able to operate as necessary. By using a Faraday Cage to shield the RF-sensitive element, it is possible to reduce its susceptibility to EMI from other systems and retain the integrity of the signal. [4] A Faraday cage is an enclosure or mesh made of conducting materials, such as copper. [5] When an electric field is applied to the cage the material particles become charged which then generates an internal field that cancels the applied fields' effect. [5]

To develop the micro-Faraday cage (MFC), HFSS can be used to create a simulation environment to design a micro-Faraday cage in an LTCC (Low-Temperature Co-fired Ceramics) substrate. Due to its physical properties and low temp firing process, LTCC allows components to be embedded within the substrate without damaging the component. To simplify the simulation and analysis process both the SMPS and the RF Sensitive components were replaced with 25 GHz antennas. An antenna can measure the effectiveness of the Faraday cage because it can detect the strength of an electromagnetic field. [8] Since a Faraday cage works by attenuating electromagnetic fields, if an antenna inside the cage detects a weaker signal than one outside the cage, it indicates that the cage is effectively blocking electromagnetic fields. [4] The value for the antenna frequency was chosen arbitrarily. The final dimensions for the substrate were 40mm x 40mm x 0.254mm. Two simulation environments were created. The first used a two-antenna system with one

transmitting and the other receiving. The second used a three-antenna system with one transmitting and two receiving.

To calculate the thickness of the Faraday cage walls to minimize material usage for fabrication the skin depth equation was used. This equation gave a thickness of 0.0004123 mm. [2,3] Skin depth is a convenient way to identify the region of a conductor in which most of the current will flow. [2,3] With skin depth, the current flowing is mostly on the surface and decays exponentially with depth through the material. [4] Because the MFC has a finite thickness, this determines how well the shield works; a thicker shield can attenuate electromagnetic fields better and to a lower frequency. [2,3,7] Since this thickness falls outside the bound's capability for fabrication so the minimum fabrication thickness of 0.0254mm (1 mil) was used instead for the outer edge of the MFC.

Honeywell Federal Manufacturing & Technologies, LLC operates the Kansas City National Security Campus for the United States Department of Energy / National Nuclear Security Administration under Contract Number DE-NA0002839

Two Antenna System - Experimental Method & Approach:

To create the testing simulation environment in HFSS, Patch Antennas were used in place of SMPS and RF components. This design consisted of two antennas, a transmitting (Tx) and receiving (Rx) pair. The transmitting antenna was placed at the top of the substrate and the receiving antenna was shielded and embedded within the LTCC material as shown below.

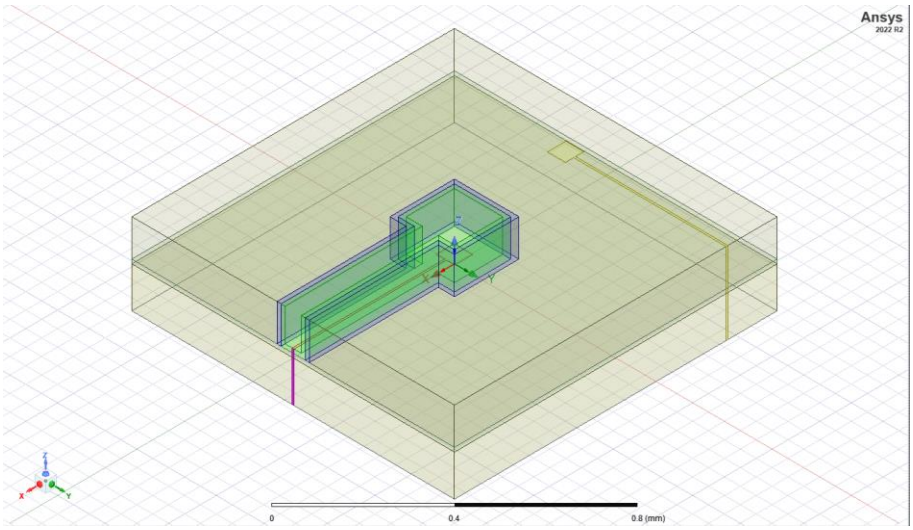

Figure 1. Dual Antenna System V1

In Figure 1 above, the antenna at the top of the substrate is the transmitting antenna. The embedded antenna in the middle and within the substrate is the receiving antenna. The chosen design for the antenna was a microstrip patch antenna due to its simple design. The patch design was made by referencing [8]. The blue material around the receiving antenna is the Faraday cage made of copper and the inner material, dubbed “Core Material”, was assigned an arbitrary dielectric constant value of $\kappa = 5$. The purpose of this material was to allow the top metallization layer of the micro-Faraday cage to be deposited without the worry of collapse should the design be fabricated.

Two Antenna System – Development & Discussion

The dual antenna system created shown in Figure 1 proved too large to simulate in HFSS with preliminary sweeps taking over 3 days of continuous running. The initial height of the substrate was set to 10 mm, but the total height had to be cut down to 10 mils for the sake of time and to keep within the limits of the fabrication in the future. After resizing the original design, the setup in Figure 2 was the result. The final dimensions were 40mm x 40mm x 0.254mm.

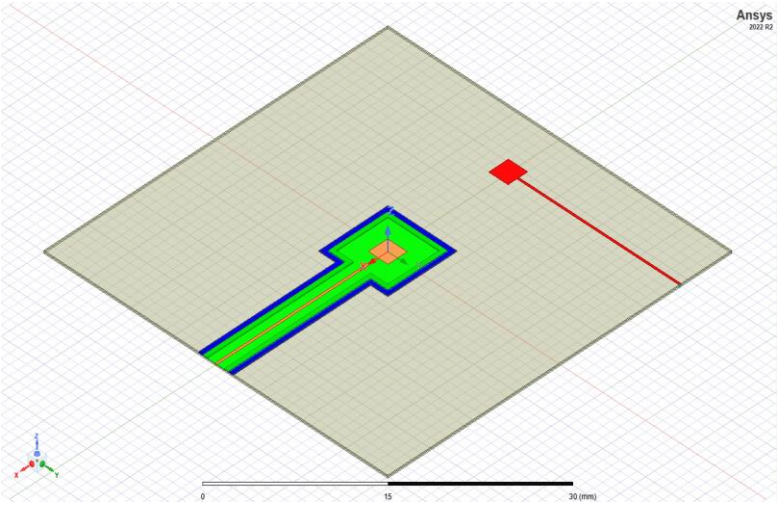

Figure 2. Dual Antenna System V10 - Revised

In Figure 2, the red antenna at the top of the substrate is the transmitting antenna. The orange antenna near the center and within the substrate is the receiving antenna. With the structure built, the next step was to simulate in HFSS to determine if the antennas were coupling as intended and if the transmission antenna was radiating at the proper frequency. Port 1 was assigned to the receiving antenna and port 2 was assigned to the transmitting antenna; This would make the forward transfer gain S(1,2). Usually, port 1 would be assigned to the port from where the signal emerges and port 2 would be where the signal is applied. The S(1,2) forward transfer gain or transmission coefficient for the antenna system in Figure 2 is shown below.

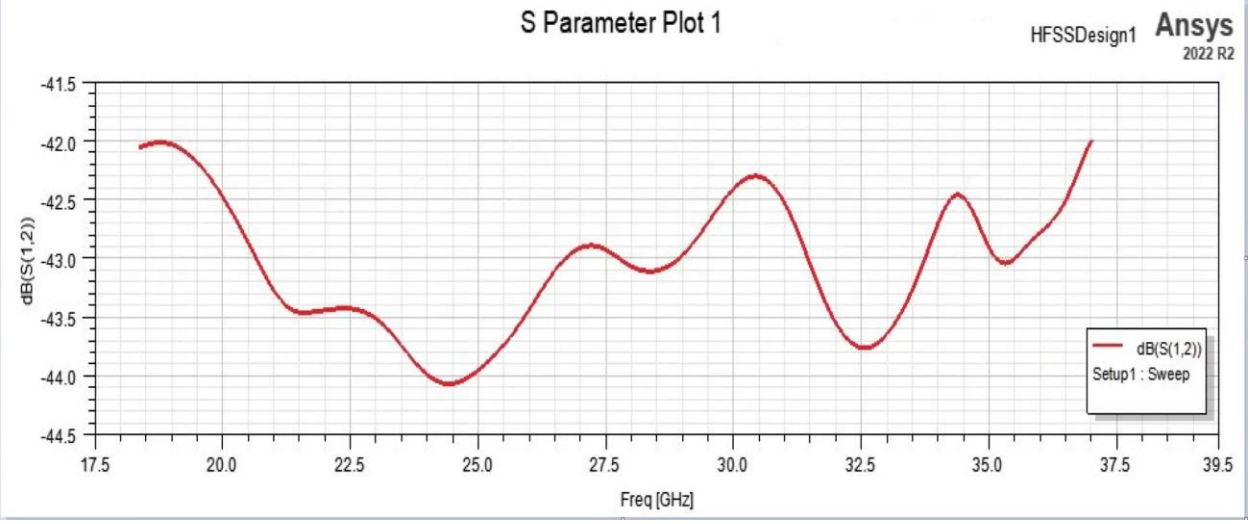

Figure 3. V10 S(1,2) Forward Transfer Gain

Although the forward gain, S(1,2), did have a dip near 25GHz, the signal itself was unstable across the entire sweep. Because of this no significant conclusion could be inferred from the plot and so another sweep was run on a larger range with all S-Parameters.

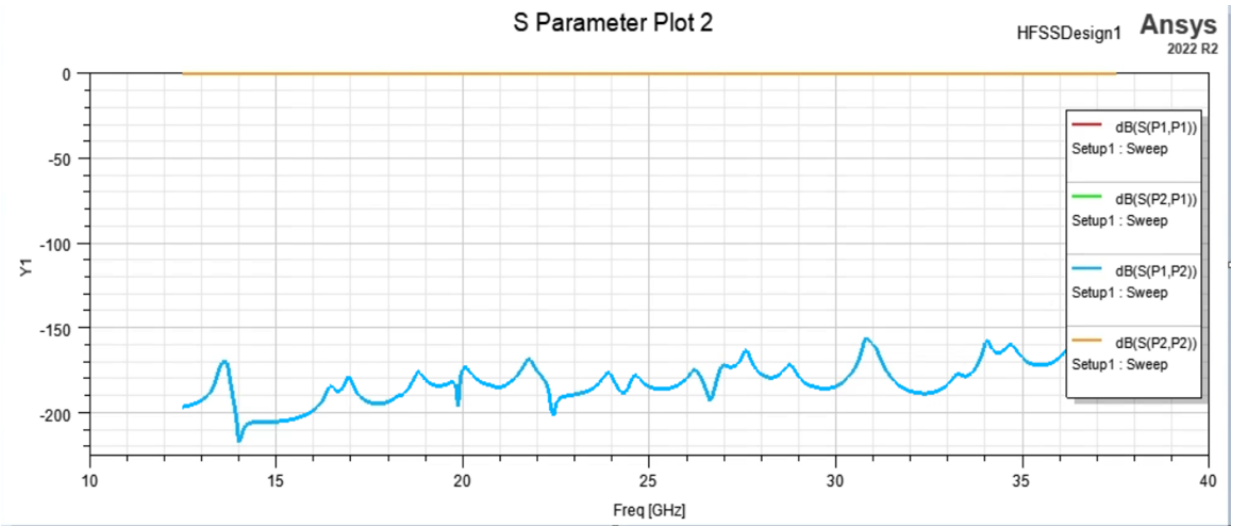

Figure 4. V10 S-Parameters Sweep

The graph in Figure 4 contains the S(1,1), S(1,2), S(2,1), and S(2,2) parameters. Even on the larger frequency range the transmission coefficient, S(1,2) remained unstable and the reflection coefficient remained unaffected at 0 dB leaving S(1,1) and S(2,1) inconclusive. More simulations were run with different settings, however, all results produced similar

waveforms to the graph above making them inconclusive since no real interpretation could be drawn from the data.

One oversight that occurred during previous simulations was a warning stating that the feedline and radiation boundary were overlapping but since no showstoppers occurred the simulations continued. Shortening the feedline from the edge helped correct the inconsistency as shown in the following S(1,2) graph.

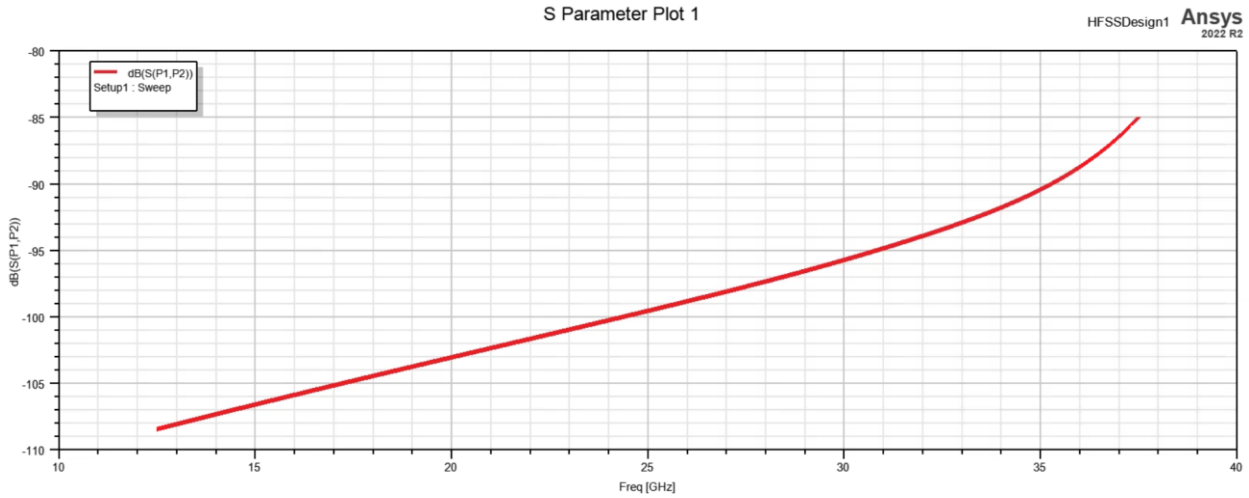

Figure 5. S(1,2) Revised Feedline Gain

This change produced a forward gain graph with a more stable trend however the graph was still incorrect as there was no formation over the 25GHz range. After this, the next step was to focus on one antenna. The purpose of this was to get the transmission antenna to radiate properly by itself and then apply similar settings to the receiving antenna to develop the two-patch system. At this point in the experiment, an important characteristic of the antenna had been overlooked, the impedance-matching inset feed. Impedance matching is important because it helps reduce the reflections in the system. [8] The reflections were high since the feedline had an impedance of 50 Ohm and the edge of the patch antenna had an impedance of over 350 Ohm. After correcting this issue, the new single transmission patch antenna produced the following results.

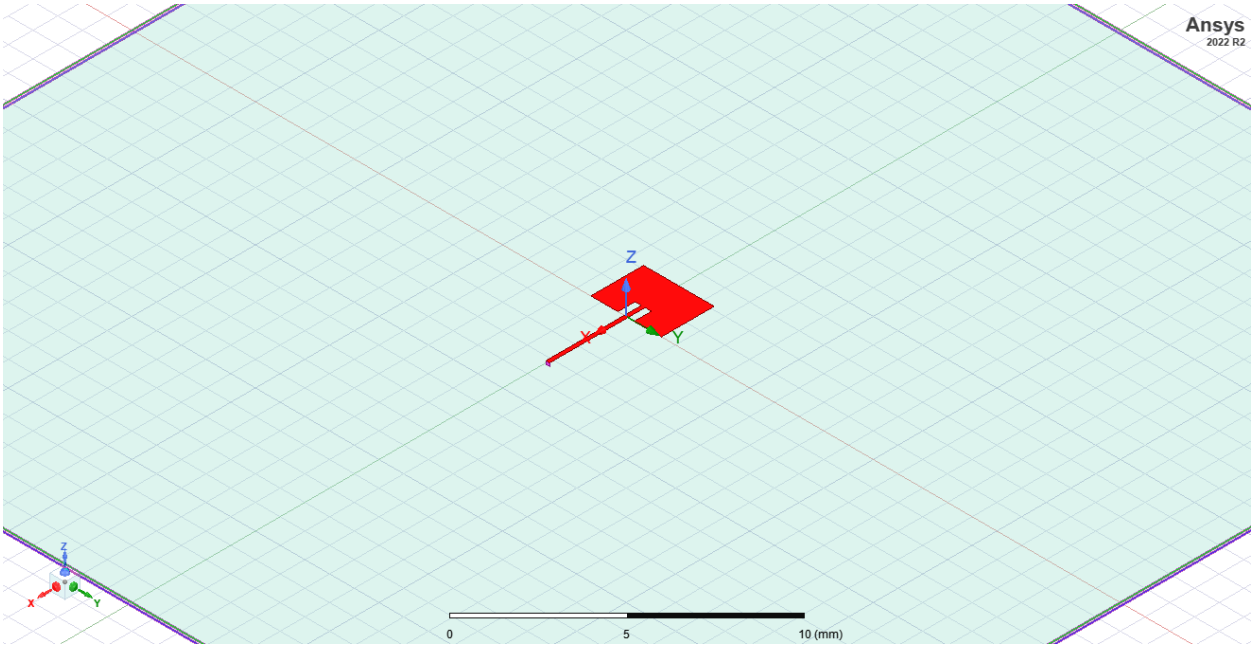

Figure 6. Patch Redesign

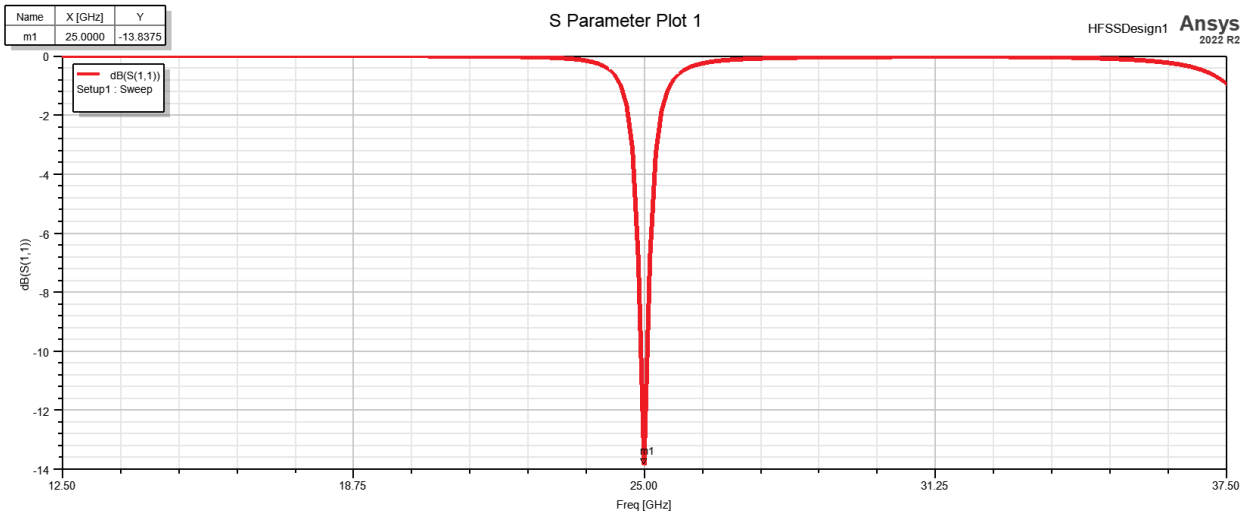

Figure 7. Single Patch Antenna S(1,1)

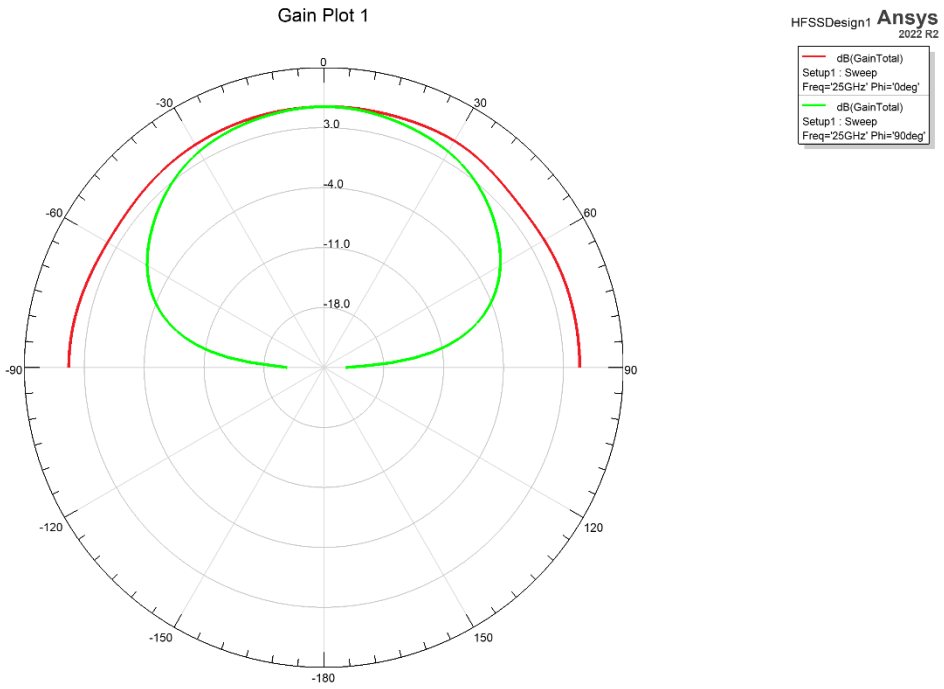

Figure 8. 2D Polar Graph

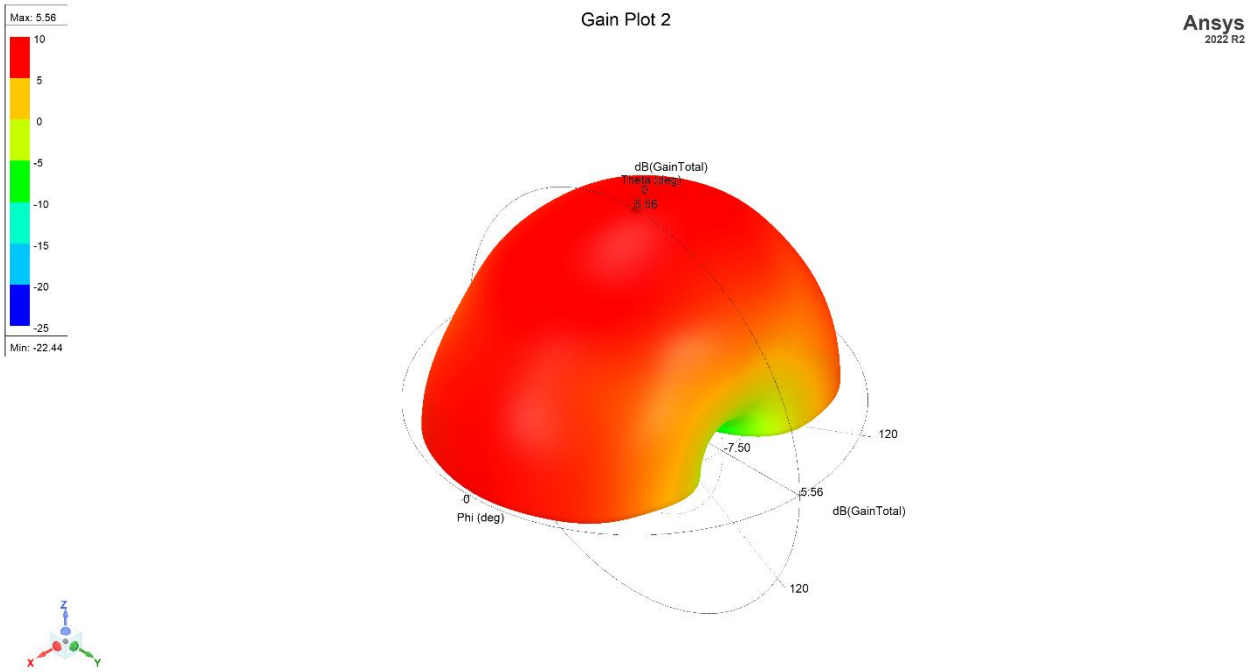

Figure 9. 3D Radiation Pattern

The improved transmission antenna design is shown in Figure 6 on top of an LTCC substrate within HFSS. From the plot in Figure 7, the new gain value was found to be-13.8dB at the resonance frequency of 25GHz. The radiation pattern in Figure 9 demonstrates the antenna now has a proper radiation field. This is further supported by the 2D radiation plot in Figure 8 which shows the 2D graph of the electromagnetic field at Phi = 0 and 90 degrees. With the antenna now radiating properly, it was then swapped into the original two-antenna system and the following figures were produced.

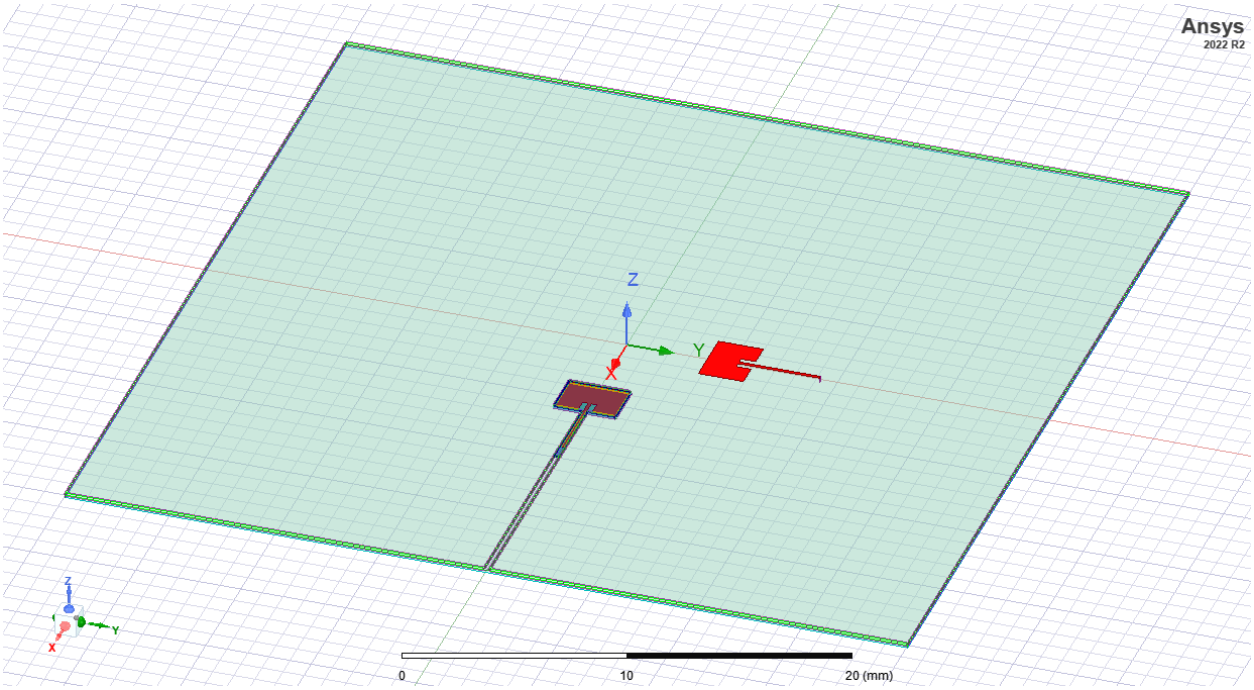

Figure 10. Two-Antenna System

The image in Figure 10 demonstrates the positioning of the two antennas. The receiving antenna is still red however the receiving antenna is now a maroon color. This is due to the green coloring of the inner core material and the blue coloring of the Faraday copper cage surrounding the entire structure. Unlike the previous two-antenna design in Figure 2, this design has noticeably thinner shielding and inner material wall with the thickness of each material being 0.0254mm (1 mil).

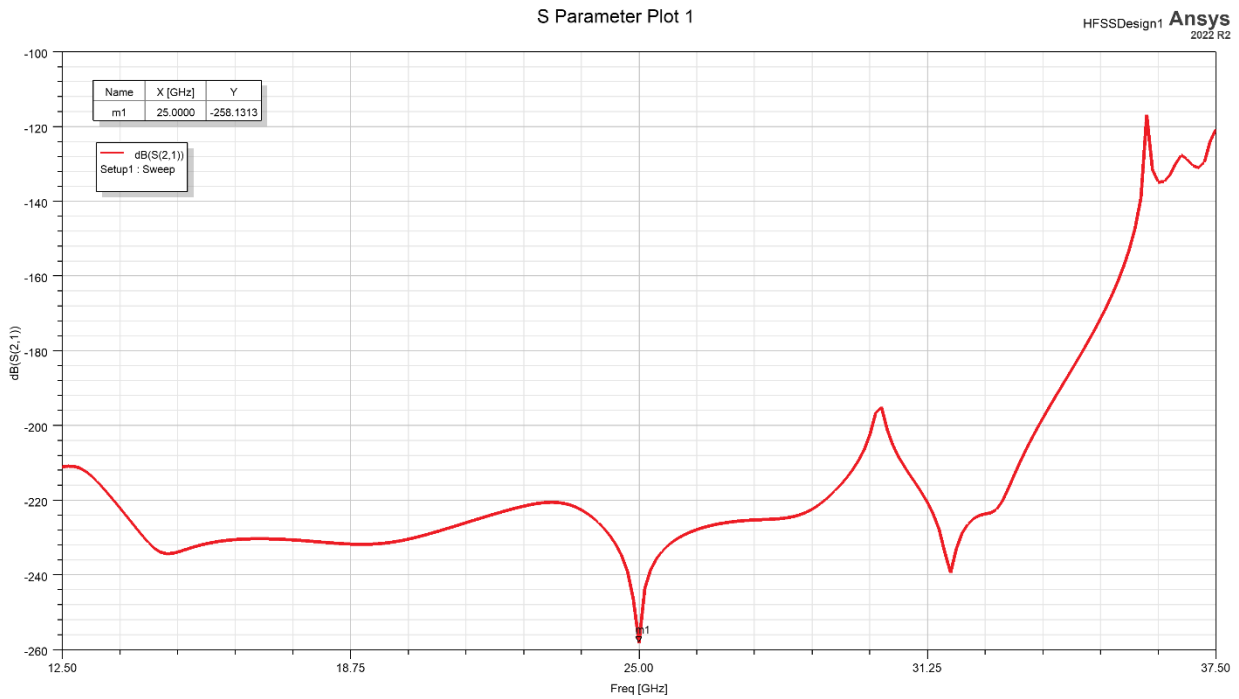

Figure 11. Two- Antenna System S(2,1) Gain

The plot in Figure 11 shows the S(2,1) plot for the two-antenna system. S(2,1) represents the power transferred from Port 1(transmitting antenna) to Port 2(receiving antenna) in a two-port network with the magnitude of S(2,1) indicates how much power is transferred from Port 1 to Port 2. [2,3,8] In the plot above the loss of the system from port 1 to port 2 was -258 dB. Although some irregularities are present, this is to be expected as the distance between the antenna positions could place the antennas within their respective near fields.

Three Antenna System - Results and Discussion:

Over the course of the experiment, it was decided that a third antenna would be added to the design. This third antenna will be another receiving antenna whose purpose will be to provide a reference for the effectiveness of the micro-Faraday cage. To create the three-antenna system a second receiving antenna was mirrored over the Y axis, so it lies opposite the shielded antenna to maintain symmetry. The transmitting antenna was left in the same spot. The three-antenna system and its results are shown in the following Figures.

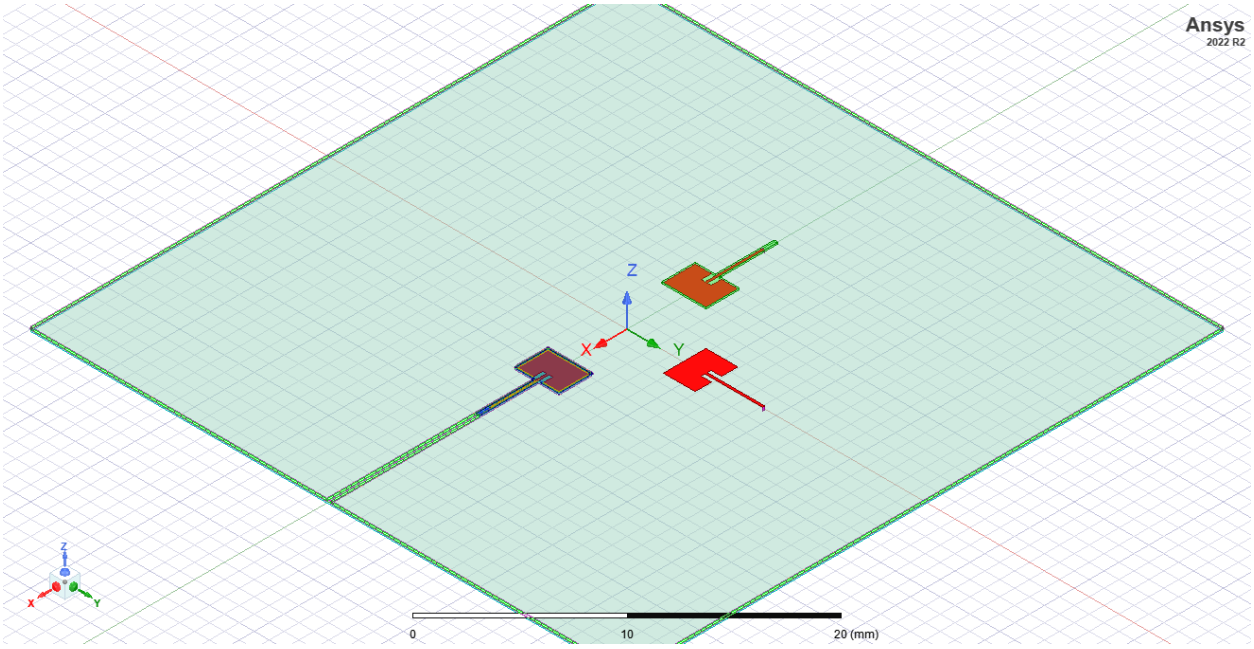

Figure 12. Three-Antenna System

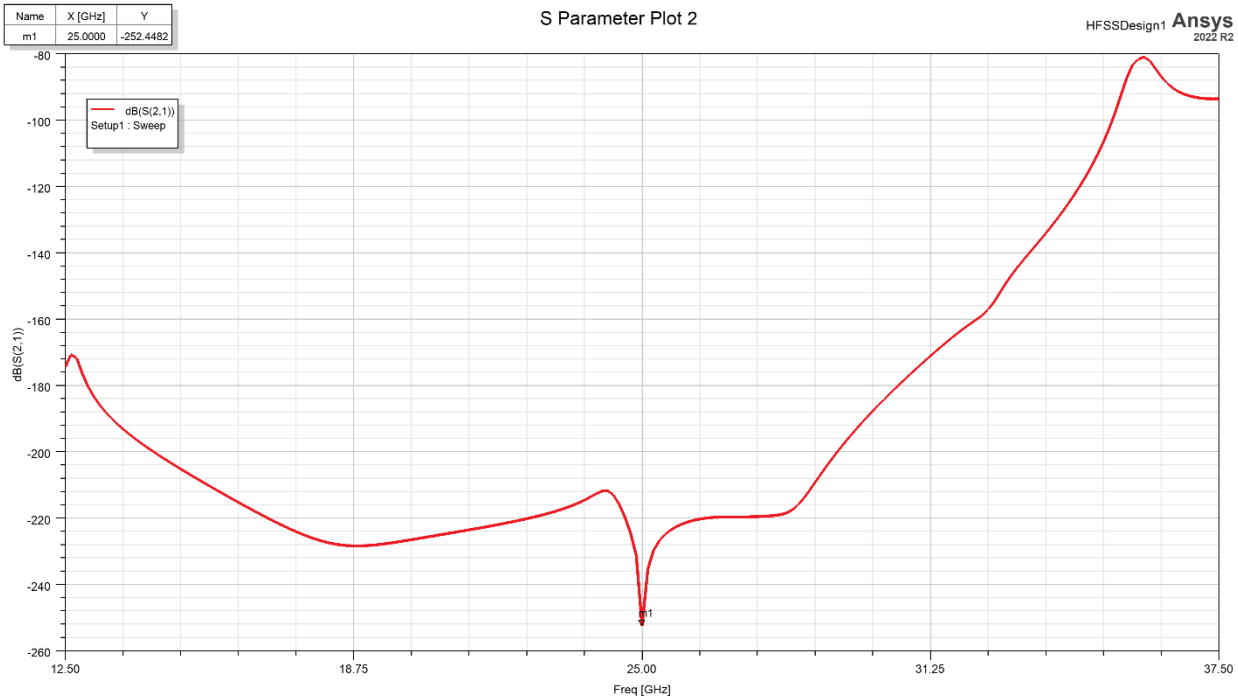

Figure 13. Three-Antenna System S(2,1) Gain

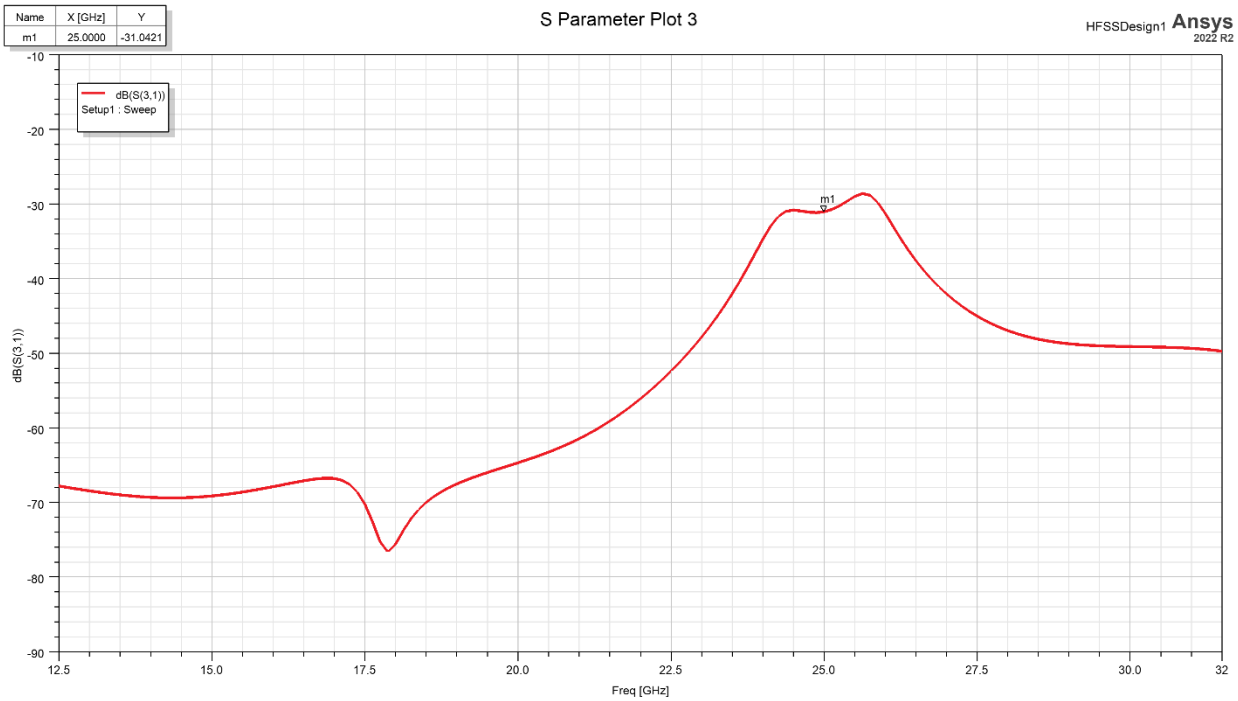

Figure 14. Three-Antenna System S(3,1) Gain

The three-antenna design is shown in Figure 12. The third antenna was assigned port 3 and was given an orange color to help distinguish it from the other two. The green material surrounding the antenna is the core material with the same dimensions as the total cage surrounding the other receiving antenna. Port 1 and port 2 assignments remained the same from the two-antenna system. The S21 plot in Figure 13 shows the loss to be -252 dB. This loss is consistent with the loss of -256dB from the two antenna S(2,1) simulation. In contrast, the S(3,1) plot in Figure 14 reveals the loss to be significantly less at only -31 dB from port 1 to port 3.

Conclusion:

Ultimately the Dual Patch antenna system helped provide a basis on which to create the three-patch antenna system. The initial figures revealed the S parameter plots for the preliminary dual patch design to be inconclusive. After altering the feedline, the forward transmission performance improved for the system, but an entire patch antenna redesign was required. After providing adequate radiation results the final patch design was used in the Dual and Triple Patch Design. From the data in this report, the Micro Faraday cage was shown to attenuate the signal by over -250 dB in both two and three antenna systems when compared to the antenna that was surrounded only by the core material which only experienced a loss of -31 dB. This data shows promising results for the effectiveness of the MFC however before an affirmative decision can be made on the Micro-Faraday Cage's effectiveness more trials need to be done using different cage configurations and alternate antenna positioning. An alternative design for the Faraday cage would be to use a mesh-style design. Another alternative design would be to place two additional transmitting antennas parallel to the receiving antennas in the Three-Antenna system. A few errors encountered throughout this experiment were some limitations in the software capability when creating the structure and assigning boundaries. These created challenges when designing or processing data, however over time these issues were resolved. As this research is still in its early stages more work is required before a finalized simulation environment is created. The ultimate objective is to replace the antenna with IC components, such as SMPS/ Power Chips or RF chips. Since this research is part of a larger Radar Consortium, the final design will utilize collaboration with other universities within the Consortium for fabrication and thermal management of power chips, such as with Michigan State University and their 3D metal printer for the Faraday cage development and the University of Nebraska- Lincoln and their diamond heatsinks for thermal management.

References:

[1] Analog Devices, “An Introduction to Switch-Mode Power Supplies,” Maxim Engineering Journal, vol. 61, pp. 14–17, 2007.

[2] D. M. Pozar, Microwave Engineering. Hoboken, Nj: Wiley, 2012.

[3] F. T. Ulaby and Umberto Ravaioli, Fundamentals of applied electromagnetics. Boston: Pearson, 2015.

[4] J. -D. V. Hoang, R. Darveaux, T. Lobianco, Y. Liu, and W. Nguyen, "Breakthrough Packaging Level Shielding Techniques and EMI Effectiveness Modeling and Characterization," 2016 IEEE 66th Electronic Components and Technology Conference (ECTC), Las Vegas, NV, USA, 2016, pp. 1290-1296, doi: 10.1109/ECTC.2016.300.

[5] M. Sørensen, S. K. Christensen, C. Vittarp and H. Ebert, "Investigation of the Workbench Faraday Cage Method, IEC 61967-5," 2021 IEEE International Joint EMC/SI/PI and EMC Europe Symposium, Raleigh, NC, USA, 2021, pp. 480-485, doi: 10.1109/EMC/SI/PI/EMCEurope52599.2021.9559285.

[6] R. Getz and B. Moeckel, “Understanding and Eliminating EMI in Microcontroller Applications.” Texas Instruments, Dallas, Aug. 1996

[7] S. W. Ellingson, “Wave Propagation in General Media,” in Electromagnetics, Blacksburg, VA: Virginia Tech Publishing, 2020

[8] Warren L. Stutzman, Gary A. Thiele, Antenna Theory & Design, Third Edition, John Wiley & Sons, Inc., 2012.